Breast Cancer Detection Using High-Density Flexible Electrode Arrays and Electrical Impedance Tomography

Matthew S. Campisi, *Member,IEEE,* Curtis Barbre, Aditya Chola, Gisselle Cunningham, Virginia Woods, and Jonathan Viventi, *Member, IEEE*

Abstract — **While mammography remains the gold standard for breast cancer screening, additional adjunctive tools for early detection of breast cancer are needed especially for young women, women with dense breast tissue and those at increased risk due to genetic factors. These patient populations, along with those populations for whom mammography is not readily available, require alternative technologies capable of effectively detecting breast cancer.**

One such adjunctive modality for breast cancer detection is Electrical Impedance Tomography (EIT). It is a non-invasive technique that measures tissue conductivity by injecting a small current through a surface electrode while measuring electrode voltage(s). The surface measurements are then used to reconstruct a conductivity mapping of the tissue. The difference in conductivities between healthy tissue and that of carcinoma enable EIT to detect cancer. Electrical Impedance Tomography does not subject the patient to ionizing radiation, and offers significant potential for detecting very small tumors in early stages of development at a low cost. While prior systems have demonstrated success using EIT for breast cancer detection, the resolution of the reconstructed image was limited by the spatial resolution of the sensing electrode array. Here, we report the use of higher density (3mm spacing) flexible micro-electrode arrays to obtain tissue impedance maps. Accurate EIT reconstruction is highly dependent on the spatial resolution and fidelity of the surface measurements. High-density, flexible arrays that conform to the breast surface can offer great potential in reconstructing higher resolution conductivity maps than have been previously achieved.

I. INTRODUCTION

Breast cancer is a leading cause of cancer-related deaths among women around the world [1], [2]. While traditional screening tools exist, additional adjunctive modalities can fill an unmet need. In particular, young women with dense breast tissue and those at higher risk due to genetic factors may benefit from additional adjunctive screening tools [3]. The large numbers of women in these high-risk populations highlight the emergent and critical need for accurate, safe, pain-free and cost-effective adjunctive breast examination tools. While MRI and mammograms provide accurate and sensitive diagnostic information, these modalities are expensive, require highly trained technicians, and are simply unavailable to many women, especially in the developing world (Fig. 1). These issues highlight the different requirements for screening tools as opposed to diagnostic tools. Effective screening tools demand low cost, easy use and a readily accessible modality that is easily interpreted.

EIT offers these benefits [4]. As a screening tool, EIT can be implemented to maximize specificity, resulting in a low false-positive rate. Rather than replacing established diagnostic modalities, an affordable and easy to interpret measurement tool may reduce the number of unnecessary biopsies performed.

The technical basis for EIT relies on injecting a small electric current through a non-invasive surface electrode and recording the corresponding voltage response over a range of signal frequencies. This stimulate-and-record foundation permits the calculation of the complex tissue conductance/impedance at each electrode. The conductance of malignant tumors significantly differs from that of benign tissue: approximately 35 microSiemens/mm for healthy breast tissue and 3-4 times higher for carcinoma at 1 kHz [5]. The impedance difference is more pronounced at higher frequencies, peaking at approximately 1 MHz [5].
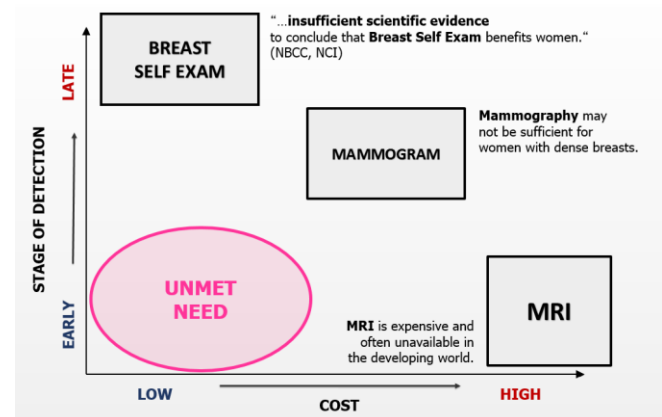

Fig. 1: Current standard breast screening modalities highlighting the unmet need for low cost, early detection adjunctive screening tools.

After acquiring the surface voltages and currents, reconstruction algorithms are used to generate a 2-D or 3-D image of the breast tissue conductivity. With a finite set of surface elements, this reconstruction (inverse problem) is ill-posed, making accurate reconstruction difficult [6]. Even so, existing EIT systems such as the TransScan 2000 have been implemented for breast cancer detection and have reported sensitivity and specificity of approximately 90% and 77% respectively [7]. It is logical that better spatial resolution of conductivity measurements on the surface may lead to a more accurate and more sensitive reconstruction of tissue conductivity. High-density flexible micro-electrode arrays with sub-millimeter electrode spacing have the capability of measuring tissue impedance across the 1 kHz – 1 MHz range at a much finer spatial resolution, potentially detecting cancerous tumors as small as 1 mm^3.

II. Implementation

The EIT system seen in Fig. 2 consisted of several hardware and software components. A flexible electrode array was placed on the surface of a tissue phantom. The array was interfaced to a set of multiplexers that select the required stimulation electrodes. The voltage and current measurement hardware provided the current stimulation circuitry and data acquisition. Current was injected from the current source, through the multiplexer and into the selected surface electrode. The logic controller selects the active multiplexer channels and scans through the array. The logic controller also synchronizes the measurements of voltage and current. The corresponding electrode voltage information is saved for subsequent offline reconstruction.
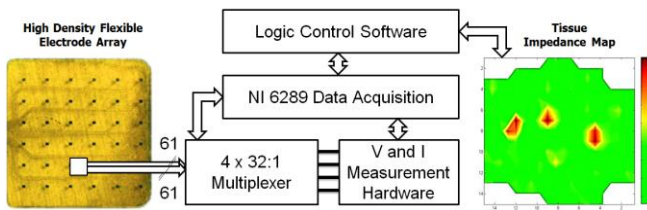

Fig. 2: EIT system block diagram. A high-density flexible electrode array is connected to multiplexers that select electrodes to connect to the current sources. Logic Control Software implemented in MATLAB controls the data acquisition hardware (National Instruments) and the multiplexers. Custom circuit provides the current (I) source and voltage (V) measurements needed to construct the impedance map.
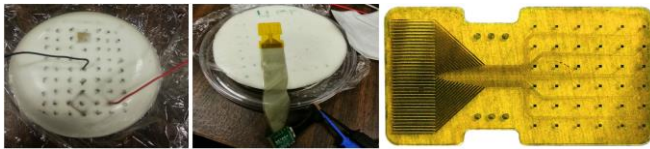

Fig. 3: (Left) Traditional electrode array with 1 cm spacing on tissue phantom. (Center) High-density (3mm pitch) flexible electrode array on tissue phantom. (Right) High-density array close-up. Electrode contacts are 400 μm x 400 μm.

A. Phantom Construction

In lieu of physiologic breast tissue, breast tissue phantoms were constructed with the electrical properties typical of adipose and cancerous tissue. Tumors measuring 1 cm^3 were fabricated and embedded in the phantom. Fig. 3 shows the constructed phantom with embedded tumors (marked on surface of the phantom). The phantoms were constructed using previously published recipes [8]. These tumors were solidified and embedded at known locations in the phantom adipose tissue to mimic the occurrence of cancer. The phantoms used for this study contained 1 or 2 malignant tumors and impedance maps were normalized against homogeneous adipose tissue control phantoms, or those with benign tumors of the same size.

B. Hardware Setup

The high-density, flexible polyimide micro-electrode arrays are connected to a multiplexing head stage printed circuit board (Fig. 4), allowing high resolution data acquisition from 61 electrodes through a single micro-HDMI connection.

The stimulation hardware consisted of a Howland constant current source coupled to four 32:1 multiplexers. The multiplexers were grouped into two banks. Each bank connected to all 61 electrodes, providing two independent pathways to connect to every electrode contact. The multiplexer configuration was designed to enable bipolar stimulation (one electrode source, one electrode sink or ground) between any pair of electrodes, or unipolar stimulation with a distant ground serving as the return, and voltage measurement on any electrode. Five address bits programmed each bank of multiplexers.

Electrode potentials were buffered using op-amps (OPA2209, Texas Instruments) and the actual current delivered to the electrodes was measured using a 50 ohm resistor in series with each constant current source output. The potential across the resistor was measured using an instrumentation amplifier (LT1168, Linear Technology) with a gain of 200. Voltages were sampled at 250 kS/s using an 18-bit analog to digital converter (USB-6289, National Instruments). Sinusoidal stimulation signals were generated at 1 MS/s using a 16-bit digital to analog converter integrated in the same data acquisition system (USB-6289, National Instruments).
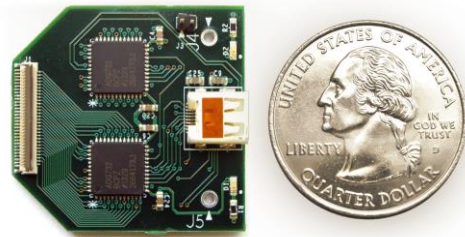

Fig. 4: Top side of quad 32:1 Mux. Routes up to four signal channels from electrode array to data acquisition hardware providing full mesh connectivity across the electrode array.

The high-density micro-electrode array used for these experiments had 400 μm x 400 μm platinum contacts, in a 3 mm spaced 6 x 6 grid. While the 1 cm^3 tumor was able to be imaged in one sweep of all electrodes on the high-density array, the array had to be carefully translated across the surface of the phantom to achieve full coverage and then stitched together in post-processing. Additionally, an industry standard low-density array with 1 cm spaced, 4 mm diameter electrode contacts was used for comparison purposes (Fig. 3, Left).

III. Methods

A. Impedance Calculation

All data acquisition and analysis was performed in MATLAB using the data acquisition toolbox session interface. The stimulation current was a sinusoidal signal at an amplitude of 10 μA operating at either 1 kHz or 100 kHz. Both voltage and current measurements were made over a period of 0.1 seconds at each electrode, relative to a single ground on the adjacent electrode. The arrays (both low density (LD) and high-density (HD)) were traversed along each row, beginning with stimulating electrode {0,0} while

grounding {0,1} ({row,col}). We then proceeded to stimulate {0,1} while grounding {0,2}, continuing this pattern until the edge of the array was reached. The same measurements were repeated on the remaining rows. After recording the data from each electrode pair, we analyzed the impedance characteristics. This procedure was completed for phantoms with no tumors, one centrally located tumor, and two adjacent tumors.

In order to calculate the complex impedance, accurate measurements of both magnitude and phase of the current and voltage were required. These measurements were extracted using spectral analysis of the measured voltage and current signals. This process consisted of taking single samples of the FFTs of the voltage and current measurements, and calculating the complex impedance at an electrode as indicated in (1).

$$Z_e = \frac{\sum_{n=0}^{L-1} V_n e^{-\left(j2\pi\frac{f}{f_s}n\right)}}{\sum_{n=0}^{L-1} I_n e^{-\left(j2\pi\frac{f}{f_s}n\right)}} \qquad (1)$$

Here Z_e was the impedance at a particular electrode; V_n and I_n were the voltage and current signal vectors. L was the padded length of the FFTs, chosen to contain an integer number of signal cycles to prevent spectral leakage in the FFT. The values f and f_s are the signal frequency and sampling rate respectively. This analysis was similar to the demodulation scheme used in [9]. The analysis above is advantageous because it minimizes effects of DC and transient voltages, as well as frequencies other than the frequency of interest. This also minimizes the effect of broadband noise. These computations can be readily implemented on a low power mobile device to enable a small, portable breast cancer screening system.

B. Impedance Mapping

After obtaining the complex impedance at each electrode, a smoothed 2-D normalized impedance map was created in MATLAB using standard image interpolation. These maps were then compared to the known phantom data.

IV. PRELIMINARY RESULTS

The normalized relative impedance at each site was mapped to 2-D images shown in Figs. 5, 6, 7, 8, and 9. These figures are a visual representation of the impedance magnitude of phantoms with malignant tumors relative to adipose tissue phantoms. Lower impedance (blue) denotes a malignant phantom tumor, and the higher impedance region (red) is normal adipose phantom tissue. Figs. 5 and 8 are control adipose phantom data for standard and high-density arrays, respectively. Figs. 6 and 7 represent measurements made with a standard low density array, while Fig. 9 was generated from data acquired with the high-density array. We observed a larger difference between the tumor and non-tumor regions of the high resolution gradient image (0.31 HD, 0.25 LD) and lower standard deviation within both regions (0.099 HD, 0.15 LD), indicating a higher signal to noise ratio. A smaller transition region between tumor and

non-tumor regions measured by the high-density array suggests a higher resolution image.

All results correlated spatially with the documented phantoms. These surface impedance maps will provide the foundation for full 3-D tomographic reconstructions in future work.

V. DISCUSSION

Preliminary results have shown the capability to measure impedances across a high-density micro-electrode array. Phantom tumors were successfully detected and differentiated from normal tissue on the basis of impedance. The low impedance tumor regions identified had impedance differences from the surrounding tissue greater than the standard deviation in impedance at the tumor site, both in magnitude and phase at 1 kHz and 100 kHz. At higher frequencies (>100 kHz) our measurement hardware introduced an additional capacitive artifact, possibly caused by the distant location of the Howland current source circuit with respect to the array, which altered the impedance measurements. This limited our measurements to a maximum frequency of 100 kHz. We will continue to investigate and reduce the unwanted capacitance.
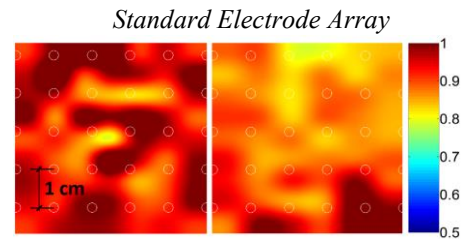
Standard Electrode Array

Fig. 5: Stitched control impedance data for the standard (1 cm) spacing EIT array.
(Left) Impedance map of all adipose phantom (no tumors) at 1 kHz.
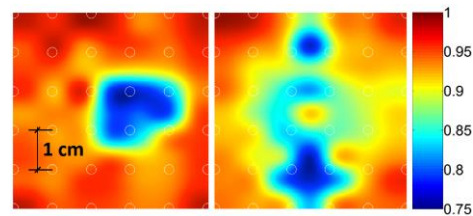(Right) Impedance map of all adipose phantom (no tumors) at 100 kHz.

Fig. 6: Normalized relative impedance maps measured using a low density (1 cm) electrode array and a 1 kHz signal. Identified tumors have lower impedance indicated in blue. Benign tissue has higher impedance indicated in red. Left image shows a single centralized tumor. Right image has two tumors separated by 3 cm.

Fig 7: Normalized relative impedance maps measured using a low density (1 cm) electrode array and a 100 kHz signal. Identified tumors have lower impedance indicated in blue. Benign tissue has higher impedance indicated in red. Left image shows a single centralized tumor. Right image has two tumors separated by 3 cm.
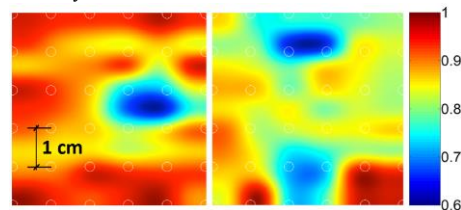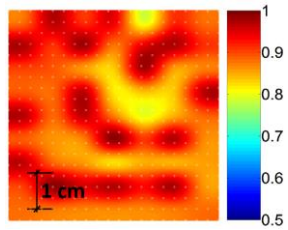
High-Density Electrode Array

Fig. 8: Control impedance data for the high-density (3 mm) spacing EIT array. Stitched impedance map of all adipose phantom (no tumors) at 1 kHz.
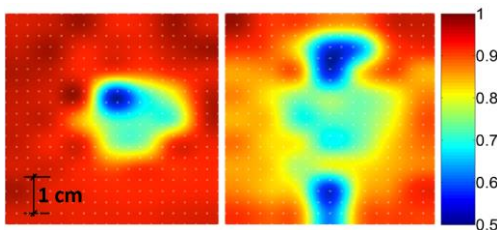

Fig. 9: Normalized relative impedance maps measured using a high-density electrode array and a 1 kHz signal. Identified tumors have lower impedance indicated in blue. Benign tissue has higher impedance indicated in red. Left image shows a single centralized tumor. Right image has two tumors separated by 3 cm.

Special consideration must be made when using high-density flexible arrays covering large spatial areas due to the large number of electrodes required. High ratio multiplexing must be used to reduce the number of physical connections to the data acquisition hardware.

Since EIT reconstruction inherently depends on a partial set of boundary voltages and current densities, it may be possible for higher resolution surface data to enable sharper reconstructions. Using sub-millimeter electrode spacing, it may be feasible to discern early-stage malignant tumors as small as 1 mm^3 immediately below the surface of the skin. In addition, detection of cancers not forming a mass, such as inflammatory breast cancer, could be within reach. Details on fabrication and implementation of a flexible micro-electrode array with sub-millimeter spacing that will be used for this purpose can be found in [10].

VI. CONCLUSION

EIT was successful in detecting phantom tumors in simulated breast tissue. Our initial results suggest that the high-density flexible electrode array not only conforms better to the tissue surface, but also provides higher resolution images.

Electrical Impedance Tomography relies on accurate phase measurement of electrode voltage relative to stimulation current. As such, stray capacitances, system delay, or undesirable frequency response in the measurement hardware limit accuracy of impedance calculations at high frequencies. We continue to both develop a model of these effects to compensate where possible, and to improve the system design to reduce the parasitic capacitances.

The development of efficient current injection patterns and reconstruction algorithms is an active area of research. Future implementation of high-density 3-D reconstructions will offer additional spatial information and clarity to doctors and clinicians. Analysis of existing reconstruction algorithms to take advantage of the high-density measurements is ongoing.

Future studies will be performed with smaller phantom tumors to assess the spatial sensitivity of the high-density electrodes. Systematic tumor depth analysis will also be investigated. While treatment options for such small tumors are still currently evolving, the outcome of this research could be revolutionary in terms of detecting early stage tumors.

REFERENCES

[1] D. M. Parkin, F. Bray, J. Ferlay and P. Pisani, "Global Cancer Statistics," A Cancer Journal for Clinicians 55, pp. 74-108, 2002.

[2] American Cancer Society Cancer Facts & Figures, 2008. http://www.cancer.org [Online].

[3] J. S. Drukteinis, B. P. Mooney, C. I. Flowers and R. A. Getenby, "Beyond mammography: new frontiers in breast cancer screening.," *The American Journal of Medicine, 126(6), 472-9. doi: 10.1016/j.amjmed.2012.11.025.,* 2013.

[4] V. Cherepenin, A. Karpov, A. Korjenevsky and V. Kornienko, "A 3D electrical imipedance tomography (EIT) system," *Physiological Measurement. 22, 9-18,* 2001.

[5] B. Sholz and R. Anderson, "On Electrical Impedance Scanning- Principles and Simulations," vol. 68, no. 1, 35-44, 2000.

[6] E. D. Holder, W. Lionheart, N. Polydorides and A. Borsic, "Methods, History and Applications, The Reconstruction Problem," vol. 0750309520, 2004.

[7] "Transcan T-Scan 2000 Gets Panel Nod As Mammography Adjunct", *The Grey Sheet,* vol. 24, no. 34, 5-6, 1998.

[8] E. Porter, J. Fakhoury, R. Oprisor, M. Coates and M. Popovi, "Improved Tissue Phantoms for Experimental Validation of Microwave Breast Cancer Detection," 2010.

[9] X. Yue and C. McLeod, "FPGA design and implementation for EIT data acquisition," *Institute of Physics and Engineering in Medicine,* no. 29, pp. 1233-1246, 2008.

[10] J. Viventi et al., "Flexible, foldable, acively multiplexed, high-density electrode array for mapping brain activity in vivo," *Nature Neuroscience,* vol. 14, pp. 1599-1605, 2011.